SIAM J. MATH. ANAL.
Vol. 48, No. 6, pp. 3962–3983
© 2016 Society for Industrial and Applied Mathematics

Downloaded 05/08/17 to 128.42.186.213. Redistribution subject to SIAM license or copyright; see http://www.siam.org/journals/ojsa.php

INVERSE BOUNDARY VALUE PROBLEM FOR THE HELMHOLTZ EQUATION: QUANTITATIVE CONDITIONAL LIPSCHITZ STABILITY ESTIMATES*

ELENA BERETTA†, MAARTEN V. DE HOOP‡, FLORIAN FAUCHER§, AND OTMAR SCHERZER¶

Abstract. We study the inverse boundary value problem for the Helmholtz equation using the Dirichlet-to-Neumann map at selected frequencies as the data. A conditional Lipschitz stability estimate for the inverse problem holds in the case of wavespeeds that are a linear combination of piecewise constant functions (following a domain partition) and gives a framework in which the scheme converges. The stability constant grows exponentially as the number of subdomains in the domain partition increases. We establish an order optimal upper bound for the stability constant. We eventually realize computational experiments to demonstrate the stability constant evolution for three-dimensional wavespeed reconstruction.

Key words. inverse problems, Helmholtz equation, stability and convergence of numerical methods

AMS subject classifications. 35R30, 86A22, 65N12, 35J25

DOI. 10.1137/15M1043856

1. Introduction.

In this paper we study the inverse boundary value problem for the Helmholtz equation using the Dirichlet-to-Neumann map at selected frequencies as the data. This inverse problem arises, for example, in reflection seismology and inverse obstacle scattering problems for electromagnetic waves [3, 22, 4]. We consider wavespeeds containing discontinuities.

Uniqueness of the mentioned inverse boundary value problem was established by Sylvester and Uhlmann [21], assuming that the wavespeed is a bounded measurable function. This inverse problem has been extensively studied from an optimization point of view. We mention, in particular, the work of [5].

It is well known that the logarithmic character of the stability of the inverse boundary value problem for the Helmholtz equation [1, 19] cannot be avoided; see also [14, 15]. In fact, in [17] Mandache proved that despite the regularity of a priori assumptions of any order on the unknown wavespeed, logarithmic stability is the best possible type. However, conditional Lipschitz stability estimates can be obtained: accounting for discontinuities, such an estimate holds if the unknown wavespeed is a finite linear combination of piecewise constant functions with an underlying known domain partitioning [6]. Such an estimate was obtained following an approach introduced by Alessandrini and Vessella [2] and further developed by Beretta and Francini

*Received by the editors October 14, 2015; accepted for publication (in revised form) September 7, 2016; published electronically November 29, 2016.
http://www.siam.org/journals/sima/48-6/M104385.html
Funding: The research of the fourth author was supported by the Austrian Science Fund (FWF), project P26687-N25 Interdisciplinary Coupled Physics Imaging.
†Dipartimento di Matematica "Brioschi," Politecnico di Milano, Milano 20133, Italy (elena.beretta@polimi.it).
‡Department of Computational and Applied Mathematics and Department of Earth Science, Rice University, Houston, TX 77005 (mdehoop@rice.edu).
§Team Project Magique-3D, INRIA Bordeaux Sud-Ouest Research Center, Pau 64000, France (florian.faucher@inria.fr).
¶Computational Science Center, University of Vienna, A-1090 Vienna, Austria (otmar.scherzer@univie.ac.at).

Copyright © by SIAM. Unauthorized reproduction of this article is prohibited.

Downloaded 05/08/17 to 128.42.186.213. Redistribution subject to SIAM license or copyright; see http://www.siam.org/journals/ojsa.php

[7] for electrical impedance tomography (EIT) based on the use of singular solutions. If, on the one hand, this method allows the use of partial data, on the other hand it does not allow one find an optimal bound of the stability constant. Here, we revisit the Lipschitz stability estimate for the full Dirichlet-to-Neumann map using complex geometrical optics (CGO) solutions which give rise to a sharp upper bound of the Lipschitz constant in terms of the number of subdomains in the domain partitioning. We develop the estimate in $L^2(\Omega)$.

Unfortunately, the use of CGO solutions leads naturally to a dependence of the stability constant on frequency of exponential type. This is clearly far from being optimal, as is also pointed out in the paper of Nagayasu, Uhlmann, and Wang [18]. There the authors prove a stability estimate in terms of Cauchy data instead of the Dirichlet-to-Neumann map using CGO solutions. They derive a stability estimate consisting of two parts: a Lipschitz stability estimate and a logarithmic stability estimate. When the frequency increases, the logarithmic part decreases while the Lipschitz part becomes dominant, but with a stability constant which blows up exponentially in frequency.

We can exploit the quantitative stability estimate via a Fourier transform in the corresponding time-domain inverse boundary value problem with bounded frequency data. Datchev and de Hoop [9] showed how to choose classes of nonsmooth coefficient functions, one of which is consistent with the class considered here, so that optimization formulations of inverse wave problems satisfy the prerequisites for the application of steepest descent and Newton-type iterative reconstruction methods. The proof is based on resolvent estimates for the Helmholtz equation. Thus, one can allow approximate localization of the data in selected time windows, with size inversely proportional to the maximum allowed frequency. This is of importance to applications in the context of reducing the complexity of field data. We note that no information is lost by cutting out a (short) time window, since the boundary source functions (and wave solutions), being compactly supported in frequency, are analytic with respect to time. We cannot allow arbitrarily high frequencies in the data. This restriction is reflected also in the observation by Blazek, Stolk, and Symes [8] that the adjoint equation, which appears in the mentioned iterative methods, does not admit solutions.

As part of the analysis, we study the Fréchet differentiability of the direct problem and obtain the frequency and domain partitioning dependencies of the relevant constants away from the Dirichlet spectrum. Our results hold for finite fixed frequency data including frequencies arbitrarily close to zero while avoiding Dirichlet eigenfrequencies; in view of the estimates, inherently, there is a finest scale which can be reached. Finally, we estimate the stability numerically and demonstrate the validity of the bounds, in particular in the context of reflection seismology.

2. Inverse boundary value problem with the Dirichlet-to-Neumann map as the data.

2.1. Direct problem and forward operator.

We describe the direct problem and some properties of the data, that is, the Dirichlet-to-Neumann map. We will formulate the direct problem as a nonlinear operator mapping F_ω from $L^\infty(\Omega)$ to $\mathcal{L}(H^{1/2}(\partial\Omega), H^{-1/2}(\partial\Omega))$ defined as

$$F_\omega(c^{-2}) = \Lambda_{\omega^2 c^{-2}},$$

Copyright © by SIAM. Unauthorized reproduction of this article is prohibited.

Downloaded 05/08/17 to 128.42.186.213. Redistribution subject to SIAM license or copyright; see http://www.siam.org/journals/ojsa.php

where $\Lambda_{\omega^2 c^{-2}}$ indicates the Dirichlet-to-Neumann operator. Indeed, at fixed frequency ω^2, we consider the boundary value problem

$$\begin{cases} (-\Delta - \omega^2 c^{-2}(x))u = & 0 \quad \text{in } \Omega, \\ u = & g \quad \text{on } \partial\Omega, \end{cases} \tag{1}$$

while $\Lambda_{\omega^2 c^{-2}}: \ g \to \frac{\partial u}{\partial \nu}|_{\partial\Omega}$, where ν denotes the outward unit normal vector to $\partial\Omega$. In this section, we will state some known results concerning the well-posedness of problem (1) (see, for example, [12]) and the regularity properties of the nonlinear map F_ω. We will sketch the proofs of these results because we will need to keep track of the dependencies of the constants involved on frequency. We invoke the following.

Assumption 1. There exist two positive constants B_1, B_2 such that

$$B_1 \le c^{-2} \le B_2 \quad \text{in } \Omega. \tag{2}$$

In the rest of section 2, $C = C(a, b, c, \dots)$ indicates that C depends only on the parameters $a, b, c, \dots$ and we will indicate different constants with the same letter C.

PROPOSITION 2. *Let Ω be a bounded Lipschitz domain in $\mathbb{R}^3$, $f \in L^2(\Omega)$, $g \in H^{1/2}(\partial\Omega)$, and $c^{-2} \in L^\infty(\Omega)$ satisfying Assumption 1. Then, there exists a discrete set $\Sigma_{c^{-2}} := \{\tilde{\lambda}_n \quad | \tilde{\lambda}_n > 0 \ \forall n \in \mathbb{N}\}$ such that, for every $\omega^2 \in \mathbb{C} \backslash \Sigma_{c^{-2}}$, there exists a unique solution $u \in H^1(\Omega)$ of*

$$\begin{cases} (-\Delta - \omega^2 c^{-2}(x))u = & f \quad \text{in } \Omega, \\ u = & g \quad \text{on } \partial\Omega. \end{cases} \tag{3}$$

Furthermore, there exists a positive constant C such that

$$\|u\|_{H^1(\Omega)} \le C \left(1 + \frac{\omega^2}{d(\omega^2, \Sigma_{c^{-2}})}\right) \left(\|g\|_{H^{1/2}(\partial\Omega)} + \|f\|_{L^2(\Omega)}\right), \tag{4}$$

where $C = C(\Omega, B_2)$, and $d(\omega^2, \Sigma_{c^{-2}})$ indicates the distance of ω^2 from $\Sigma_{c^{-2}}$.

Proof. We first prove the result for $g = 0$. Consider the linear operators $-\Delta : H^1_0(\Omega) \to H^{-1}(\Omega)$ and the multiplication operator

$$\begin{aligned} M_{c^{-2}} : L^2(\Omega) &\to L^2(\Omega), \\ u &\to c^{-2} u, \end{aligned} \tag{5}$$

respectively. We can now consider the operator $K = \Delta^{-1} M_{c^{-2}} : H^1_0(\Omega) \to H^1_0(\Omega)$. The equation

$$(-\Delta - \omega^2 c^{-2}(x))u = f$$

for $u \in H^1_0(\Omega)$ is equivalent to

$$(I - \omega^2 K)u = \Delta^{-1} f. \tag{6}$$

Note that $K : H^1_0(\Omega) \to H^1_0(\Omega)$ is compact by the Rellich–Kondrachov compactness theorem. Furthermore, by Assumption 1 and the properties of Δ^{-1}, it follows that K is self-adjoint and positive. Hence, K has a discrete set of positive eigenvalues $\{\alpha_n\}_{n \in \mathbb{N}}$ such that $\alpha_n \to 0$ as $n \to \infty$. Let $\tilde{\lambda}_n := \frac{1}{\alpha_n}, n \in \mathbb{N}$, define $\Sigma_{c^{-2}} := \{\tilde{\lambda}_n \ : \ n \in \mathbb{N}\}$, and let $\omega^2 \in \mathbb{C} \backslash \Sigma_{c^{-2}}$, and show that it satisfies the assumptions of this proposition. Then, by the Fredholm alternative, there exists a unique solution $u \in H^1_0(\Omega)$ of (6).

Copyright © by SIAM. Unauthorized reproduction of this article is prohibited.

Downloaded 05/08/17 to 128.42.186.213. Redistribution subject to SIAM license or copyright; see http://www.siam.org/journals/ojsa.php

To prove estimate (4), we observe that

$$u = \sum_{n=1}^{\infty} \langle u, e_n \rangle e_n, \quad Ku = \sum_{n=1}^{\infty} \alpha_n \langle u, e_n \rangle e_n,$$

where $\{e_n\}_{n\in\mathbb{N}}$ is an orthonormal basis of $L^2(\Omega)$. Hence we can rewrite (6) in the form

$$\sum_{n=1}^{\infty} (1 - \omega^2 \alpha_n) \langle u, e_n \rangle e_n = \sum_{n=1}^{\infty} \langle h, e_n \rangle e_n, \text{ where } h = \Delta^{-1} f.$$

Hence,

$$\langle u, e_n \rangle = \frac{1}{1 - \frac{\omega^2}{\tilde{\lambda}_n}} \langle h, e_n \rangle \quad \forall n \in \mathbb{N}$$

and

$$u = \sum_{n=1}^{\infty} \frac{1}{1 - \frac{\omega^2}{\tilde{\lambda}_n}} \langle h, e_n \rangle e_n$$

so that

$$\|u\|_{L^2(\Omega)} \leq \left(1 + \frac{\omega^2}{d(\omega^2, \Sigma_{c^{-2}})}\right) \|h\|_{L^2(\Omega)} \leq C \left(1 + \frac{\omega^2}{d(\omega^2, \Sigma_{c^{-2}})}\right) \|f\|_{L^2(\Omega)}, \tag{7}$$

where $C = C(\Omega, B_2)$.

Now, by multiplying (3) with u, integrating by parts, and using Schwartz' inequality, Assumption 1, and (7) it follows in the case $g = 0$ that

$$\|\nabla u\|_{L^2(\Omega)} \leq C \left(1 + \frac{\omega^2}{d(\omega^2, \Sigma_{c^{-2}})}\right) \|f\|_{L^2(\Omega)}. \tag{8}$$

Hence, by (7) and (8) we finally get

$$\|u\|_{H^1(\Omega)} \leq C \left(1 + \frac{\omega^2}{d(\omega^2, \Sigma_{c^{-2}})}\right) \|f\|_{L^2(\Omega)}.$$

If g is not identically zero, then we reduce the problem to the previous case by considering $v = u - \tilde{g}$, where $\tilde{g} \in H^1(\Omega)$ is such that $\tilde{g} = g$ on $\partial\Omega$ and $\|\tilde{g}\|_{H^1(\Omega)} \leq \|g\|_{H^{1/2}(\partial\Omega)}$, and we derive easily the estimate

$$\|u\|_{H^1(\Omega)} \leq C \left(1 + \frac{\omega^2}{d(\omega^2, \Sigma_{c^{-2}})}\right) (\|f\|_{L^2(\Omega)} + \|g\|_{H^{1/2}(\partial\Omega)}),$$

which concludes the proof. ◻

The constants appearing in the estimate of Proposition 2 depend on c^{-2} and $\Sigma_{c^{-2}}$, which are unknown. To our purposes it would be convenient to have constants depending only on a priori parameters B_1, B_2 and other known parameters. Let us denote by Σ_0 the spectrum of $-\Delta$. Then, we have the following.

PROPOSITION 3. *Suppose that the assumptions of Proposition 2 are satisfied. Let $\{\lambda_n\}_{n\in\mathbb{N}}$ denote the Dirichlet eigenvalues of $-\Delta$. Then, for any $n \in \mathbb{N}$,*

$$\frac{\lambda_n}{B_2} \leq \tilde{\lambda}_n \leq \frac{\lambda_n}{B_1}. \tag{9}$$

Copyright © by SIAM. Unauthorized reproduction of this article is prohibited.

If ω^2 is such that

$$0 < \omega^2 < \frac{\lambda_1}{B_2}, \tag{10}$$

or, for some $n \geq 1$,

$$\frac{\lambda_n}{B_1} < \omega^2 < \frac{\lambda_{n+1}}{B_2}, \tag{11}$$

then there exists a unique solution $u \in H^1(\Omega)$ of problem (1) *and the following estimate holds:*

$$\|u\|_{H^1(\Omega)} \leq C \left(\|g\|_{H^{1/2}(\partial\Omega)} + \|f\|_{L^2(\Omega)} \right),$$

where $C = C(B_1, B_2, \omega^2, \Sigma_0)$.

Proof. To derive estimate (9), we consider the Rayleigh quotient related to (1):

$$\frac{\int_\Omega |\nabla v|^2}{\int_\Omega c^{-2} v^2}.$$

By Assumption 1, for any nontrivial $v \in H_0^1(\Omega)$, we have

$$\frac{1}{B_2} \frac{\int_\Omega |\nabla v|^2}{\int_\Omega v^2} \leq \frac{\int_\Omega |\nabla v|^2}{\int_\Omega c^{-2} v^2} \leq \frac{1}{B_1} \frac{\int_\Omega |\nabla v|^2}{\int_\Omega v^2} \ .$$

Now, we apply the Courant–Rayleigh minimax principle (see for instance [10, Theorem 4.5.1], where the infinite-dimensional Courant–Rayleigh minimax principle has been considered). The following arguments are similar to those in the simple one-dimensional example of Davies' book [10, Example 4.6.1]. Due to Assumption 1, the Hilbert space

$$L_c^2(\Omega) = \left\{ v : \int_\Omega c^{-2} v^2 < \infty \right\}$$

with norm $\|v\|_{L_c^2} = \int_\Omega v^2 c^{-2}$ is equivalent to $L^2(\Omega)$:

$$\tilde{\lambda}_n := \inf_{\{\tilde{u}_1,\ldots,\tilde{u}_n \in H_0^1(\Omega)\}} \sup_{v \in \text{span}\{\tilde{u}_1,\ldots,\tilde{u}_n\} : \|v\|_{L_c^2} \leq 1} \frac{\int_\Omega |\nabla v|^2}{\int_\Omega c^{-2} v^2} \, ,$$

$$\lambda_n := \inf_{\{u_1,\ldots,u_n \in H_0^1(\Omega)\}} \sup_{v \in \text{span}\{u_1,\ldots,u_n\} : \|v\|_{L^2} \leq 1} \frac{\int_\Omega |\nabla v|^2}{\int_\Omega v^2} \ .$$

Note that $\|v\|_{L^2} \leq 1$ implies that $\|v\|_{L_c^2}^2 \leq B_2$ and that $L_c^2(\Omega) = L^2(\Omega)$. Therefore,

$$\lambda_n \leq \inf_{\{u_1,\ldots,u_n \in H_0^1(\Omega)\}} \sup_{v \in \text{span}\{u_1,\ldots,u_n\} : \|v\|_{L_c^2}^2 \leq B_2} \frac{\int_\Omega |\nabla v|^2}{\int_\Omega v^2} \ .$$

Now, using the scale invariance of $\frac{\int_\Omega |\nabla v|^2}{\int_\Omega v^2}$ and the fact that $c^{-2} \leq B_2$, we get

$$\lambda_n \leq B_2 \inf_{\{u_1,\ldots,u_n \in H_0^1(\Omega)\}} \sup_{v \in \text{span}\{u_1,\ldots,u_n\} : \|v\|_{L_c^2} \leq 1} \frac{\int_\Omega |\nabla v|^2}{\int_\Omega c^{-2} v^2} = B_2 \tilde{\lambda}_n \ .$$

Copyright © by SIAM. Unauthorized reproduction of this article is prohibited.

Downloaded 05/08/17 to 128.42.186.213. Redistribution subject to SIAM license or copyright; see http://www.siam.org/journals/ojsa.php

Downloaded 05/08/17 to 128.42.186.213. Redistribution subject to SIAM license or copyright; see http://www.siam.org/journals/ojsa.php

To get the lower bound estimate for $\tilde{\lambda}_n$, observe that if $\|v\|_{L^2_c} \le 1$, then $\|v\|^2_{L^2} \le \frac{1}{B_1}$. Hence,

$$\tilde{\lambda}_n \le \inf_{\{\tilde{u}_1,\dots,\tilde{u}_n \in H^1_0(\Omega)\}} \sup_{v \in \mathrm{span}\{\tilde{u}_1,\dots,\tilde{u}_n\}: \|v\|^2_{L^2} \le \frac{1}{B_1}} \frac{\int_\Omega |\nabla v|^2}{\int_\Omega c^{-2} v^2} .$$

Now, using the scale invariance of $\frac{\int_\Omega |\nabla v|^2}{\int_\Omega v^2}$ and the fact that $c^{-2} \ge B_1$, we get

$$\tilde{\lambda}_n \le \inf_{\{\tilde{u}_1,\dots,\tilde{u}_n \in H^1_0(\Omega)\}} \sup_{v \in \mathrm{span}\{\tilde{u}_1,\dots,\tilde{u}_n\}: \|v\|_{L^2} \le 1} \frac{\int_\Omega |\nabla v|^2}{\int_\Omega c^{-2} v^2} = \frac{1}{B_1} \lambda_n .$$

Thus we have shown that

$$\frac{\lambda_n}{B_2} \le \tilde{\lambda}_n \le \frac{\lambda_n}{B_1} \quad \forall n \in \mathbb{N}.$$

Hence, we have well-posedness of problem (1) if we select an ω^2 satisfying (10) or (11) and the claim follows. ∎

We observe that in order to derive the uniform estimates of Proposition 3 we need to assume that either the frequency is small (10) or that the oscillation of c^{-2} is sufficiently small (11). This observation can also been found in Davies' book [10].

In the seismic application we have in mind, we might know the spectrum of some reference wavespeed c_0^{-2}. The following local result holds.

PROPOSITION 4. *Let Ω and c_0^{-2} satisfy the assumptions of Proposition 2 and let $\omega^2 \in \mathbb{C} \backslash \Sigma_{c_0^{-2}}$, where $\Sigma_{c_0^{-2}}$ is the Dirichlet spectrum of (1) corresponding to c_0^{-2}. Then there exists $\delta = \delta(\Omega, \omega^2, B_2, \Sigma_{c_0^{-2}}) > 0$ such that, if*

$$\|c^{-2} - c_0^{-2}\|_{L^\infty(\Omega)} \le \delta,$$

then $\omega^2 \in \mathbb{C} \backslash \Sigma_{c^{-2}}$ and the solution u of problem (3) corresponding to c^{-2} satisfies

$$\|u\|_{H^1(\Omega)} \le C \left(1 + \frac{\omega^2}{d(\omega^2, \Sigma_{c_0^{-2}})} \right) \left(\|f\|_{L^2(\Omega)} + \|g\|_{H^{1/2}(\partial\Omega)} \right), \quad C = C(\Omega, B_2).$$

Proof. Let $\delta_c := c^{-2} - c_0^{-2}$ and consider $u_0 \in H^1(\Omega)$ the unique solution of (3) for c_0^{-2}. Consider the problem

$$\begin{cases} -\Delta v - \omega^2 c_0^{-2} v - \omega^2 \delta_c v = & \omega^2 u_0 \delta_c \quad \text{in } \Omega, \\ v = & 0 \quad \text{on } \partial\Omega. \end{cases} \tag{12}$$

Let now

$$L := -\Delta - \omega^2 c_0^{-2};$$

then, by assumption, it is invertible from $H^1_0(\Omega)$ to $L^2(\Omega)$ and we can rewrite problem (12) in the form

$$(I - K)v = h, \tag{13}$$

where $K = \omega^2 L^{-1} M_{\delta_c}$ and M_{δ_c} is the multiplication operator defined in (5) and $h = L^{-1}(\omega^2 u_0 \delta_c)$. Observe now that from (4), $\|L^{-1}\| \le C(1 + \frac{\omega^2}{d_0})$ with $C = C(\Omega, B_2)$ and where $d_0 = \mathrm{dist}(\omega^2, \Sigma_{c_0^{-2}})$. Hence, we derive

$$\|K\| \le \omega^2 \|L^{-1}\| \|M_{\delta_c}\| \le \omega^2 \|L^{-1}\| \delta \le C\omega^2 \left(1 + \frac{\omega^2}{d_0} \right) \delta.$$

Copyright © by SIAM. Unauthorized reproduction of this article is prohibited.

Hence, choosing $\delta = \frac{1}{2}(C\omega^2(1+\frac{\omega^2}{d_0}))^{-1}$, the bounded operator K has norm smaller than one. Hence, $I-K$ is invertible and there exists a unique solution v of (13) in H_0^1 satisfying (4) with $C = C(B_2, \omega^2, \Omega, d_0)$, and since $u = u_0 + v$ the statement follows. ∎

Let ω^2 be such that either

$$0 < \omega^2 < \frac{\lambda_1}{B_2},$$

or, for some $n \geq 1$,

$$\frac{\lambda_n}{B_1} < \omega^2 < \frac{\lambda_{n+1}}{B_2},$$

and let

$$\mathcal{W} := \{c^{-2} \in L^\infty(\Omega) : B_1 \leq c^{-2} \leq B_2\}\,.$$

Then the direct operator

$$\begin{aligned} F_\omega : \mathcal{W} &\to \mathcal{L}(H^{1/2}(\partial\Omega), H^{-1/2}(\partial\Omega)),\\ c^{-2} &\mapsto \Lambda_{\omega^2 c^{-2}} \end{aligned}$$

is well defined.

We will examine the regularity properties of F_ω in the following lemmas. We will show the Fréchet differentiability of it.

LEMMA 5 (Fréchet differentiability). *Let $c^{-2} \in L^\infty(\Omega)$ satisfy Assumption* 1. *Assume that $\omega^2 \in \mathbb{C}\backslash\Sigma_{c^{-2}}$. Then, the direct operator F_ω is Fréchet differentiable at c^{-2} and its Fréchet derivative $DF_\omega(c^{-2})$ satisfies*

$$\|DF_\omega[c^{-2}]\|_{\mathcal{L}(L^\infty(\Omega),\mathcal{L}(H^{1/2}(\partial\Omega),H^{-1/2}(\partial\Omega)))} \leq C\omega^2\left(1+\frac{\omega^2}{d(\omega^2,\Sigma_{c^{-2}})}\right)^2, \tag{14}$$

where $C = C(\Omega, B_2)$.

Proof. Consider $c^{-2} + \delta c^{-2}$. Then, from Proposition 4, if $\|\delta c^{-2}\|_{L^\infty}(\Omega)$ is small enough, $\omega^2 \notin \Sigma_{c^{-2}+\delta c^{-2}}$. An application of Alessandrini's identity then gives

$$\left\langle \left(\Lambda_{\omega^2(c^{-2}+\delta c^{-2})} - \Lambda_{\omega^2 c^{-2}}\right) g\,,\, h\right\rangle = \omega^2 \int_\Omega \delta c^{-2}\, uv\,\mathrm{d}x, \tag{15}$$

where $\langle\cdot,\cdot\rangle$ is the dual pairing with respect to $H^{-1/2}(\partial\Omega)$, and $H^{1/2}(\partial\Omega)$, and u and v solve the boundary value problems

$$\begin{cases} (-\Delta - \omega^2(c^{-2}+\delta c^{-2}))u = & 0, \quad x\in\Omega,\\ u = & g, \quad x\in\partial\Omega, \end{cases}$$

and

$$\begin{cases} (-\Delta - \omega^2 c^{-2})v = & 0, \quad x\in\Omega,\\ v = & h, \quad x\in\partial\Omega, \end{cases}$$

respectively. We first show that the map F_ω is Fréchet differentiable and that the Fréchet derivative is given by

$$\langle DF_\omega[c^{-2}](\delta c^{-2})g\,,\, h\rangle = \omega^2 \int_\Omega \delta c^{-2}\,\tilde{u}v\,\mathrm{d}x, \tag{16}$$

Copyright © by SIAM. Unauthorized reproduction of this article is prohibited.

Downloaded 05/08/17 to 128.42.186.213. Redistribution subject to SIAM license or copyright; see http://www.siam.org/journals/ojsa.php

Downloaded 05/08/17 to 128.42.186.213. Redistribution subject to SIAM license or copyright; see http://www.siam.org/journals/ojsa.php

where $\tilde{u}$ solves the equation

$$\begin{cases} (-\Delta - \omega^2 c^{-2})\tilde{u} = 0, & x \in \Omega, \\ \tilde{u} = g, & x \in \partial\Omega. \end{cases}$$

In fact, by (15), we have that

$$\langle (\Lambda_{\omega^2(c^{-2}+\delta c^{-2})} - \Lambda_{\omega^2 c^{-2}})g\,,\, h\rangle - \omega^2 \int_\Omega \delta c^{-2}\, \tilde{u} v \,\mathrm{d}x = \omega^2 \int_\Omega \delta c^{-2}\,(u-\tilde{u})v\,\mathrm{d}x. \tag{17}$$

We note that $u - \tilde{u}$ solves the equations

$$\begin{cases} (-\Delta - \omega^2 c^{-2})(u-\tilde{u}) = -\omega^2 \delta c^{-2}\, u, & x \in \Omega, \\ u - \tilde{u} = 0, & x \in \partial\Omega. \end{cases}$$

Using the fact that $u-\tilde{u}$ and v are in $H^1(\Omega)$ and that $\delta c^{-2} \in L^\infty(\Omega)$, and applying the Cauchy–Schwarz inequality, we get

$$\left|\omega^2 \int_\Omega \delta c^{-2}\,(u-\tilde{u})v\,\mathrm{d}x\right| \le \omega^2 \|\delta c^{-2}\|_{L^\infty(\Omega)} \|u-\tilde{u}\|_{L^2(\Omega)} \|v\|_{L^2(\Omega)}. \tag{18}$$

Finally, using the stability estimates of Proposition 2 applied to $u - \tilde{u}$ and to v, and the stability estimates of Proposition 4 applied to u, we derive

$$\begin{aligned} &\left|\omega^2 \int_\Omega \delta c^{-2}\,(u-\tilde{u})v\,\mathrm{d}x\right| \\ &\quad \le C\omega^4 \left(1 + \frac{\omega^2}{\mathrm{d}(\omega^2, \Sigma_{c^{-2}})}\right)^3 \|\delta c^{-2}\|^2_{L^\infty(\Omega)} \|g\|_{H^{1/2}(\partial\Omega)} \|h\|_{H^{1/2}(\partial\Omega)}. \end{aligned} \tag{19}$$

Hence,

$$\begin{aligned} &\left|\langle (\Lambda_{\omega^2(c^{-2}+\delta c^{-2})} - \Lambda_{\omega^2 c^{-2}})g\,,\, h\rangle - \omega^2 \int_\Omega \delta c^{-2}\, \tilde{u} v\,\mathrm{d}x\right| \\ &\quad \le C\omega^4 \left(1 + \frac{\omega^2}{\mathrm{d}(\omega^2, \Sigma_{c^{-2}})}\right)^3 \|\delta c^{-2}\|^2_{L^\infty(\Omega)} \|g\|_{H^{1/2}(\partial\Omega)} \|h\|_{H^{1/2}(\partial\Omega)}, \end{aligned}$$

which proves differentiability.

Finally, by

$$\langle DF_\omega[c^{-2}](\delta c^{-2})g\,,\, h\rangle = \omega^2 \int_\Omega \delta c^{-2}\, \tilde{u} v\,\mathrm{d}x,$$

we get

$$\begin{aligned} \left|\langle DF_\omega[c^{-2}](\delta c^{-2})g\,,\, h\rangle\right| &\le \omega^2 \|\delta c^{-2}\|_{L^\infty(\Omega)} \|\tilde{u}\|_{L^2(\Omega)} \|v\|_{L^2(\Omega)} \\ &\le \omega^2 \left(1 + \frac{\omega^2}{\mathrm{d}(\omega^2, \Sigma_{c^{-2}})}\right)^2 \|\delta c^{-2}\|_{L^\infty(\Omega)} \|g\|_{H^{1/2}(\partial\Omega)} \|h\|_{H^{1/2}(\partial\Omega)}, \end{aligned}$$

from which (14) follows. ∎

2.2. Conditional quantitative Lipschitz stability estimate. Let B_2, r_0, r_1, A, L, N be positive with $N \in \mathbb{N}, N \ge 2$, $r_0 < 1$. In the following we will refer to these numbers as we did to the a priori data. To prove the results of this section we invoke the following common assumptions.

Copyright © by SIAM. Unauthorized reproduction of this article is prohibited.

Downloaded 05/08/17 to 128.42.186.213. Redistribution subject to SIAM license or copyright; see http://www.siam.org/journals/ojsa.php

Assumption 6. $\Omega \subset \mathbb{R}^3$ is a bounded domain such that

$$|x| \leq Ar_1 \quad \forall x \in \Omega.$$

Moreover,

$$\partial\Omega \text{ is of Lipschitz class with constants } r_1 \text{ and } L.$$

Let $\mathcal{D}_N$ be a partition of Ω given by

$$\mathcal{D}_N \triangleq \left\{ \{D_1, D_2, \dots, D_N\} \mid \bigcup_{j=1}^{N} \overline{D}_j = \Omega \;,\; (D_j \cap D_{j'})^\circ = \emptyset, j \neq j' \right\} \tag{20}$$

such that

$$\{\partial D_j\}_{j=1}^N \text{ is of Lipschitz class with constants } r_0 \text{ and } L.$$

Assumption 7. The function $c^{-2} \in \mathcal{W}_N$; that is, it satisfies

$$B_1 \leq c^{-2} \leq B_2 \quad \text{in } \Omega$$

and is of the form

$$c^{-2}(x) = \sum_{j=1}^{N} c_j \chi_{D_j}(x),$$

where $c_j, j = 1, \dots, N$ are unknown numbers and $\{D_1, \dots, D_N\} \in \mathcal{D}_N$.

Assumption 8. Assume

$$0 < \omega^2 < \frac{\lambda_1}{B_2},$$

or, for some $n \geq 1$,

$$\frac{\lambda_n}{B_1} < \omega^2 < \frac{\lambda_{n+1}}{B_2}.$$

Under the above assumptions we can state the following preliminary result.

LEMMA 9. *Let Ω and $\mathcal{D}_N$ satisfy Assumption 6 and let $c^{-2} \in \mathcal{W}_N$. Then, for every $s' \in (0, 1/2)$, there exists a positive constant C with $C = C(L, s')$ such that*

$$\|c^{-2}\|_{H^{s'}(\Omega)} \leq C(L, s') \frac{1}{r_0^{s'}} \|c^{-2}\|_{L^2(\Omega)}. \tag{21}$$

Proof. The proof is based on the extension of a result of Magnanini and Papi in [16] to the three-dimensional setting. In fact, following the argument in [16], one has that

$$\|\chi_{D_j}\|^2_{H^{s'}(\Omega)} \leq \frac{16\pi}{(1-2s')(2s')^{1+2s'}} |D_j|^{1-2s'} |\partial D_j|^{2s'}. \tag{22}$$

We now use the fact that $\{D_j\}_{j=1}^N$ is a partition of disjoint sets of Ω to show the following inequality:

$$\|c^{-2}\|^2_{H^{s'}(\Omega)} \leq 2 \sum_{j=1}^{N} c_j^2 \|\chi_{D_j}\|^2_{H^{s'}(\Omega)}. \tag{23}$$

Copyright © by SIAM. Unauthorized reproduction of this article is prohibited.

Downloaded 05/08/17 to 128.42.186.213. Redistribution subject to SIAM license or copyright; see http://www.siam.org/journals/ojsa.php

In fact, in order to prove (23), recall that

$$\|c^{-2}\|^2_{H^{s'}(\Omega)} = \int_\Omega\int_\Omega \frac{|\sum_{j=1}^N c_j(\chi_{D_j}(x)-\chi_{D_j}(y))|^2}{|x-y|^{3+2s'}}\,dx\,dy$$

and observe that, since the $\{D_j\}_{j=1}^N$ is a partition of disjoint sets of Ω, we get

$$\left|\sum_{j=1}^N c_j(\chi_{D_j}(x)-\chi_{D_j}(y))\right|^2 = \sum_{j=1}^N c_j^2(\chi_{D_j}(x)-\chi_{D_j}(y))^2 - \sum_{i\neq j} c_i c_j \chi_{D_i}(x)\chi_{D_j}(y).$$

Again, by the fact that the $\{D_j\}_{j=1}^N$ are disjoint sets, we have

$$\begin{aligned}
\sum_{i\neq j}|c_ic_j|\chi_{D_i}(x)\chi_{D_j}(y) &\le \sum_{i\neq j}\frac{c_i^2+c_j^2}{2}\chi_{D_i}(x)\chi_{D_j}(y)\\
&= \sum_{i\neq j}\frac{c_i^2}{2}(\chi_{D_i}(x)-\chi_{D_i}(y))^2\chi_{D_i}(x)\chi_{D_j}(y)\\
&\quad + \sum_{i\neq j}\frac{c_j^2}{2}(\chi_{D_j}(x)-\chi_{D_j}(y))^2\chi_{D_i}(x)\chi_{D_j}(y)\\
&\le \sum_{i\neq j}\frac{c_i^2}{2}(\chi_{D_i}(x)-\chi_{D_i}(y))^2\chi_{D_j}(y) + \sum_{i\neq j}\frac{c_j^2}{2}(\chi_{D_j}(x)-\chi_{D_j}(y))^2\chi_{D_i}(x)\\
&\le \sum_{i=1}^N\frac{c_i^2}{2}(\chi_{D_i}(x)-\chi_{D_i}(y))^2\sum_{j=1}^N\chi_{D_j}(y) + \sum_{j=1}^N\frac{c_j^2}{2}(\chi_{D_j}(x)-\chi_{D_j}(y))^2\sum_{i=1}^N\chi_{D_i}(y)\\
&\le \sum_{i=1}^N\frac{c_i^2}{2}(\chi_{D_i}(x)-\chi_{D_i}(y))^2 + \sum_{j=1}^N\frac{c_j^2}{2}(\chi_{D_j}(x)-\chi_{D_j}(y))^2\\
&= \sum_{i=1}^N c_i^2(\chi_{D_i}(x)-\chi_{D_i}(y))^2,
\end{aligned}$$

where we have used the fact that $\sum_{i=1}^N \chi_{D_i}\le 1$. So, we have derived that

$$\left|\sum_{j=1}^N c_j(\chi_{D_j}(x)-\chi_{D_j}(y))\right|^2 \le 2\sum_{j=1}^N c_j^2(\chi_{D_j}(x)-\chi_{D_j}(y))^2,$$

from which it follows that

$$\begin{aligned}
\|c^{-2}\|^2_{H^{s'}(\Omega)} &= \int_\Omega\int_\Omega \frac{|\sum_{j=1}^N c_j(\chi_{D_j}(x)-\chi_{D_j}(y))|^2}{|x-y|^{3+2s'}}\,dx\,dy\\
&\le 2\int_\Omega\int_\Omega \frac{\sum_{j=1}^N c_j^2(\chi_{D_j}(x)-\chi_{D_j}(y))^2}{|x-y|^{3+2s'}}\,dx\,dy\\
&\le 2\sum_{j=1}^N c_j^2\int_\Omega\int_\Omega \frac{(\chi_{D_j}(x)-\chi_{D_j}(y))^2}{|x-y|^{3+2s'}}\,dx\,dy = 2\sum_{j=1}^N c_j^2\|\chi_{D_j}\|^2_{H^{s'}(\Omega)},
\end{aligned}$$

which proves (23). So, finally, from (22), (23), and Assumption 6 we get

Copyright © by SIAM. Unauthorized reproduction of this article is prohibited.

$$\|c^{-2}\|^2_{H^{s'}(\Omega)} \leq 2\sum_{j=1}^{N} c_j^2 \|\chi_{D_j}\|^2_{H^{s'}(\Omega)} \leq C(s')\sum_{j=1}^{N} c_j^2 |D_j| \left(\frac{|\partial D_j|}{|D_j|}\right)^{2s'}$$
$$\leq \frac{C(L,s')}{r_0^{2s'}}\|c^{-2}\|^2_{L^2(\Omega)}. \qquad \square$$

We are now ready to state and prove our main stability result.

PROPOSITION 10. *Assume Assumption* 6, *let* $c_1^{-1}, c_2^{-1} \in \mathcal{W}_N$, *and let* ω^2 *satisfy Assumption* 8. *Then, there exists a positive constant* K, *depending on* A, r_1, L, *such that*

(24)
$$\|c_1^{-2} - c_2^{-2}\|_{L^2(\Omega)} \leq \frac{1}{\omega^2}\, e^{K(1+\omega^2 B_2)(|\Omega|/r_0^3)^{\frac{4}{7}}}\ \|\Lambda_{\omega^2 c_1^{-2}} - \Lambda_{\omega^2 c_2^{-2}}\|_{\mathcal{L}(H^{1/2}(\partial\Omega), H^{-1/2}(\partial\Omega))}.$$

Proof. To prove our stability estimate, we follow Alessandrini's idea of using CGO solutions, but we use slightly different ones from those introduced in [21] and in [1] to obtain better constants in the stability estimates, as proposed by [11]. We also use the estimates proposed in [11] (see Theorem 4.4) and due to [13] concerning the case of bounded potentials.

In fact, by Theorem 4.3 of [11], since $c^{-2} \in L^\infty(\Omega)$, $\|c^{-2}\|_{L^\infty(\Omega)} \leq B_2$, there exists a positive constant $C = C(\omega^2, B_2, A, r_1)$ such that for every $\zeta \in \mathbb{C}^3$ satisfying $\zeta \cdot \zeta = 0$ and $|\zeta| \geq C$, the equation

$$-\Delta u - \omega^2 c^{-2} u = 0$$

has a solution of the form

$$u(x) = e^{ix\cdot\zeta}(1 + R(x)),$$

where $R \in H^1(\Omega)$ satisfies

$$\|R\|_{L^2(\Omega)} \leq \frac{C}{|\zeta|}, \quad \|\nabla R\|_{L^2(\Omega)} \leq C.$$

Let $\xi \in \mathbb{R}^3$ and let $\tilde{\omega}_1$ and $\tilde{\omega}_2$ be unit vectors of $\mathbb{R}^3$ such that $\{\tilde{\omega}_1, \tilde{\omega}_2, \xi\}$ is an orthogonal set of vectors of $\mathbb{R}^3$. Let s be a positive parameter to be chosen later and set for $k = 1, 2$,

(25)
$$\zeta_k = \begin{cases} (-1)^{k-1}\frac{s}{\sqrt{2}}\left(\sqrt{(1-\frac{|\xi|^2}{2s^2})}\tilde{\omega}_1 + (-1)^{k-1}\frac{1}{\sqrt{2}s}\xi + \mathrm{i}\tilde{\omega}_2\right) & \text{for } \frac{|\xi|}{\sqrt{2}s} < 1, \\ (-1)^{k-1}\frac{s}{\sqrt{2}}\left((-1)^{k-1}\frac{1}{\sqrt{2}s}\xi + \mathrm{i}\left(\sqrt{(\frac{|\xi|^2}{2s^2}-1)}\tilde{\omega}_1 + \tilde{\omega}_2\right)\right) & \text{for } \frac{|\xi|}{\sqrt{2}s} \geq 1. \end{cases}$$

Then a straightforward computation gives

$$\zeta_k \cdot \zeta_k = 0$$

for $k = 1, 2$ and

$$\zeta_1 + \zeta_2 = \xi.$$

Furthermore, for $k = 1, 2$,

(26)
$$|\zeta_k| = \begin{cases} s & \text{for } \frac{|\xi|}{\sqrt{2}s} < 1, \\ \frac{|\xi|}{\sqrt{2}} & \text{for } \frac{|\xi|}{\sqrt{2}s} \geq 1. \end{cases}$$

Copyright © by SIAM. Unauthorized reproduction of this article is prohibited.

Downloaded 05/08/17 to 128.42.186.213. Redistribution subject to SIAM license or copyright; see http://www.siam.org/journals/ojsa.php

Hence,

$$|\zeta_k| = \max\left\{s, \frac{|\xi|}{\sqrt{2}}\right\}. \tag{27}$$

Then, by Theorem 4.3 of [11], for $|\zeta_1|, |\zeta_2| \geq C_1 = \max\{C_0\omega^2 B_2, 1\}$, with $C_0 = C_0(A, r_1)$, there exist u_1, u_2 solutions to $-\Delta u_k - \omega^2 c_k^{-2} u_k = 0$ for $k = 1, 2$, respectively, of the form

$$u_1(x) = e^{\mathrm{i}x\cdot\zeta_1}(1 + R_1(x)), \quad u_2(x) = e^{\mathrm{i}x\cdot\zeta_2}(1 + R_2(x)) \tag{28}$$

with

$$\|R_k\|_{L^2(\Omega)} \leq \frac{C_0\sqrt{|\Omega|}}{s}\omega^2 B_2 \tag{29}$$

and

$$\|\nabla R_k\|_{L^2(\Omega)} \leq C_0\sqrt{|\Omega|}\omega^2 B_2 \tag{30}$$

for $k = 1, 2$. It is common in the literature to use estimates which contain $\sqrt{|\Omega|}$. Different estimates in terms of $|\Omega|$ are possible and just change the leading constant C_0.

Consider again Alessandrini's identity

$$\int_\Omega \omega^2(c_1^{-2} - c_2^{-2})u_1 u_2 \mathrm{d}x = \langle(\Lambda_1 - \Lambda_2)u_1|_{\partial\Omega}, u_2|_{\partial\Omega}\rangle,$$

where $u_k \in H^1(\Omega)$ is any solution of $-\Delta u_k - \omega^2 c_k^{-2} u_k = 0$ and $\Lambda_k = \Lambda_{\omega^2 c_k^{-2}}$ for $k = 1, 2$. Inserting the solutions (28) in Alessandrini's identity, we derive

$$\begin{aligned} &\left|\int_\Omega \omega^2(c_1^{-2} - c_2^{-2})e^{\mathrm{i}\xi\cdot x}\mathrm{d}x\right| \\ &\quad\leq \|\Lambda_1 - \Lambda_2\|\|u_1\|_{H^{1/2}(\partial\Omega)}\|u_2\|_{H^{1/2}(\partial\Omega)} \\ &\quad\quad + \left|\int_\Omega \omega^2(c_1^{-2} - c_2^{-2})e^{\mathrm{i}\xi\cdot x}(R_1 + R_2 + R_1R_2)\mathrm{d}x\right| \\ &\quad\leq \|\Lambda_1 - \Lambda_2\|\|u_1\|_{H^1(\Omega)}\|u_2\|_{H^1(\Omega)} \\ &\quad\quad + E(\|R_1\|_{L^2(\Omega)} + \|R_2\|_{L^2(\Omega)} + \|R_1\|_{L^4(\Omega)}\|R_2\|_{L^4(\Omega)}), \end{aligned} \tag{31}$$

where $E := \|\omega^2(c_1^{-2} - c_2^{-2})\|_{L^2(\Omega)}$. By (27), (29), and (30), and since $\Omega \subset B_{2R}(0)$, we have

$$\|u_k\|_{H^1(\Omega)} \leq C\sqrt{|\Omega|}(s + |\xi|)e^{Ar_1(s+|\xi|)}, \quad k = 1, 2.$$

Let $s \geq C_2$ so that $s + |\xi| \leq e^{Ar_1(s+|\xi|)}$. Then, for $s \geq C_3 = \max(C_1, C_2)$, using (29) and (30) and the standard interpolation inequality ($\|u\|_{L^4(\Omega)} \leq \|u\|_{L^6(\Omega)}^{3/4}\|u\|_{L^2(\Omega)}^{1/4}$), we get

$$\left|\omega^2(c_1^{-2} - c_2^{-2})\hat{\ }(\xi)\right| \leq C\sqrt{|\Omega|}\left(e^{4Ar_1(s+|\xi|)}\|\Lambda_1 - \Lambda_2\| + \frac{\omega^2 B_2 E}{s}\right), \tag{32}$$

where the $\omega^2 c_k^{-2}$'s have been extended to all $\mathbb{R}^3$ by zero and $\hat{\ }$ denotes the Fourier transform. Hence, from (32), we get

$$\int_{|\xi|\leq\rho} |\omega^2(c_1^{-2} - c_2^{-2})\hat{\ }(\xi)|^2 \mathrm{d}\xi \leq C|\Omega|\rho^3\left(e^{8Ar_1(s+\rho)}\|\Lambda_1 - \Lambda_2\|^2 + \frac{\omega^4 B_2^2 E^2}{s^2}\right)$$

Copyright © by SIAM. Unauthorized reproduction of this article is prohibited.

Downloaded 05/08/17 to 128.42.186.213. Redistribution subject to SIAM license or copyright; see http://www.siam.org/journals/ojsa.php

Downloaded 05/08/17 to 128.42.186.213. Redistribution subject to SIAM license or copyright; see http://www.siam.org/journals/ojsa.php

and hence

$$\|\omega^2(c_1^{-2}-c_2^{-2})\hat{}\|^2_{L^2(\mathbb{R}^3)} \le C|\Omega|\rho^3\left(e^{8Ar_1(s+\rho)}\|\Lambda_1-\Lambda_2\|^2+\frac{\omega^4B_2^2E^2}{s^2}\right) + \int_{|\xi|\ge\rho}|\omega^2(c_1^{-2}-c_2^{-2})\hat{}(\xi)|^2\,\mathrm{d}\xi, \tag{33}$$

where $C=C(A,r_1)$. By (21) and (23), we have that

$$\|\omega^2(c_1^{-2}-c_2^{-2})\|^2_{H^{s'}(\Omega)} \le \frac{C}{r_0^{2s'}}E^2,$$

where C depends on L, s' and hence

$$\rho^{2s'}\int_{|\xi|\ge\rho}|\omega^2(c_1^{-2}-c_2^{-2})\hat{}(\xi)|^2\,\mathrm{d}\xi \le \int_{|\xi|\ge\rho}|\xi|^{2s'}|\omega^2(c_1^{-2}-c_2^{-2})\hat{}(\xi)|^2\,\mathrm{d}\xi$$
$$\le \int_{\mathbb{R}^3}(1+|\xi|^2)^{s'}|\omega^2(c_1^{-2}-c_2^{-2})\hat{}(\xi)|^2\,\mathrm{d}\xi \le \frac{C}{r_0^{2s'}}E^2.$$

Hence, we get

$$\int_{|\xi|\ge\rho}|\omega^2(c_1^{-2}-c_2^{-2})\hat{}(\xi)|^2\,\mathrm{d}\xi \le \frac{CE^2}{r_0^{2s'}\rho^{2s'}}$$

for every $s'\in(0,1/2)$. Inserting the last bound in (33), we derive

$$\|\omega^2(c_1^{-2}-c_2^{-2})\hat{}\|^2_{L^2(\mathbb{R}^3)} \le C\left(\rho^3|\Omega|e^{8Ar_1(s+\rho)}\|\Lambda_1-\Lambda_2\|^2+\rho^3|\Omega|\frac{\omega^4B_2^2E^2}{s^2}+\frac{E^2}{r_0^{2s'}\rho^{2s'}}\right),$$

where $C=C(L,s')$. To make the last two terms in the right-hand side of the inequality of equal size, we pick up

$$\sqrt[3]{|\Omega|}\rho = \left(\frac{|\Omega|}{r_0^3}\right)^{\frac{2s'}{3(3+2s')}}\left(\frac{1}{\alpha}\right)^{\frac{1}{3+2s'}} s^{\frac{2}{3+2s'}}$$

with $\alpha=\max\{1,\omega^4B_2^2\}$. Then, by Assumption 6 and observing that we might assume without loss of generality that $|\Omega|/r_0^3>1$ (if not we can choose a smaller r_0 so that such a condition is satisfied) we obtain

$$\|\omega^2(c_1^{-2}-c_2^{-2})\|^2_{L^2(\Omega)} \le CE^2\left(\frac{|\Omega|}{r_0^3}\right)^{\frac{2s'}{3+2s'}} \times\left(e^{C_4\left(\frac{|\Omega|}{r_0^3}\right)^{\frac{2s'}{3(3+2s')}}s}\left(\frac{\|\Lambda_1-\Lambda_2\|}{E}\right)^2+\left(\frac{\alpha}{s^2}\right)^{\frac{2s'}{3+2s'}}\right)$$

for $s\ge C_3$, and where C depends on s', L, A, r_1 and C_4 depends on L, A, r_1. We now make the substitution

$$s=\frac{1}{C_4\left(\frac{|\Omega|}{r_0^3}\right)^{\frac{2s'}{3(3+2s')}}}\left|\log\frac{\|\Lambda_1-\Lambda_2\|}{E}\right|,$$

Copyright © by SIAM. Unauthorized reproduction of this article is prohibited.

Downloaded 05/08/17 to 128.42.186.213. Redistribution subject to SIAM license or copyright; see http://www.siam.org/journals/ojsa.php

where we assume that

$$\frac{\|\Lambda_1 - \Lambda_2\|}{E} < c := e^{-\bar{C}\max\{1,\omega^2 B_2\}\left(\frac{|\Omega|}{r_0^3}\right)^{\frac{2s'}{3(3+2s')}}}$$

with $\bar{C} = \bar{C}(R)$ in order that the constraint $s \geq C_3$ is satisfied. Under this assumption,

(34)

$$\|\omega^2(c_1^{-2} - c_2^{-2})\|_{L^2(\Omega)} \leq C(\sqrt{\alpha})^{\frac{2s'}{3+2s'}} \left(\frac{|\Omega|}{r_0^3}\right)^{\frac{2s'}{3+2s'}\frac{9+10s'}{6(3+2s')}} E\left(\left|\log\frac{\|\Lambda_1 - \Lambda_2\|}{E}\right|^{-\frac{2s'}{3+2s'}}\right),$$

where $C = C(L, s', A, r_1)$ and we can rewrite the last inequality in the form

$$E \leq C(1+\omega^2 B_2)^{\frac{2s'}{3+2s'}} \left(\frac{|\Omega|}{r_0^3}\right)^{\frac{2s'}{3+2s'}\frac{9+10s'}{6(3+2s')}} E\left(\left|\log\frac{\|\Lambda_1 - \Lambda_2\|}{E}\right|^{-\frac{2s'}{3+2s'}}\right), \tag{35}$$

which gives

$$E \leq e^{C(1+\omega^2 B_2)\left(\frac{|\Omega|}{r_0^3}\right)^{\frac{9+10s'}{6(3+2s')}}} \|\Lambda_1 - \Lambda_2\|, \tag{36}$$

where $C = C(L, s', A, r_1)$. On the other hand, if

$$\frac{\|\Lambda_1 - \Lambda_2\|}{E} \geq c,$$

then

$$\|\omega^2(c_1^{-2} - c_2^{-2})\|_{L^2(\Omega)} \leq c^{-1}\|\Lambda_1 - \Lambda_2\| \leq e^{\bar{C}(1+\omega^2 B_2)\left(\frac{|\Omega|}{r_0^3}\right)^{\frac{1}{3(3+2s')}}} \|\Lambda_1 - \Lambda_2\|. \tag{37}$$

Hence, from (36) and (37), and recalling that $s' \in \left(0, \frac{1}{2}\right)$, we have that

$$E \leq e^{C(1+\omega^2 B_2)\left(\frac{|\Omega|}{r_0^3}\right)^{\frac{9+10s'}{6(3+2s')}}} \|\Lambda_1 - \Lambda_2\|. \tag{38}$$

Choosing $s' = \frac{1}{4}$, we derive

$$\|c_1^{-2} - c_2^{-2}\|_{L^2(\Omega)} \leq \frac{1}{\omega^2} e^{K(1+\omega^2 B_2)(|\Omega|/r_0^3)^{\frac{4}{7}}} \|\Lambda_1 - \Lambda_2\|,$$

where $K = K(L, A, r_1, s')$ and the claim follows. ∎

Remark 11. Here we state an L^∞-stability estimate, in contrast to the L^2-stability estimate in Proposition 10.

Observing that

$$\frac{1}{\sqrt{|\Omega|}}\|c_1^{-2} - c_2^{-2}\|_{L^2(\Omega)} \leq \|c_1^{-2} - c_2^{-2}\|_{L^\infty(\Omega)} \leq \frac{C}{r_0^{3/2}}\|c_1^{-2} - c_2^{-2}\|_{L^2(\Omega)},$$

where $C = C(L)$, we immediately get the following stability estimate in the L^∞ norm:

$$\|c_1^{-2} - c_2^{-2}\|_{L^\infty(\Omega)} \leq \frac{C}{\omega^2} e^{K(1+\omega^2 B_2)(|\Omega|/r_0^3)^{\frac{4}{7}}} \|\Lambda_1 - \Lambda_2\|$$

with $C = C(L)$.

Copyright © by SIAM. Unauthorized reproduction of this article is prohibited.

Downloaded 05/08/17 to 128.42.186.213. Redistribution subject to SIAM license or copyright; see http://www.siam.org/journals/ojsa.php

Remark 12. In [6] the following lower bound of the stability constant has been obtained in the case of a uniform polyhedral partition $\mathcal{D}_N$:

$$C_N \geq \frac{1}{4\omega^2} e^{K_1 N^{\frac{1}{5}}}. \tag{39}$$

Choose a uniform cubical partition $\mathcal{D}_N$ of Ω of mesh size r_0. Then,

$$|\Omega| = N r_0^3 \tag{40}$$

and estimate (24) of Proposition 10 gives

$$C_N = \frac{1}{\omega^2} e^{K(1+\omega^2 B_2) N^{\frac{4}{7}}}, \tag{41}$$

which proves a sharp bound on the Lipschitz constant with respect to N when the global Dirichlet-to-Neumann map is known. In [6] a Lipschitz stability estimate has been derived in terms of the local Dirichlet-to-Neumann map using singular solutions. These types of solution allow one to recover the unknown piecewise constant wavespeed by determining it on the outer boundary of the domain and then, by propagating the singularity inside the domain, to recover step by step the wavespeed on the interface of all subdomains of the partition. This iterative procedure does not lead to sharp bounds of the Lipschitz constant appearing in the stability estimate. It would be interesting if one could get a better bound of the Lipschitz constant using oscillating solutions.

Remark 13. In Lemma 5, we have seen that F_ω is Fréchet differentiable with Lipschitz derivative DF_ω, for which we have derived an upper bound in terms of the a priori data. From the stability estimates we can easily derive the following lower bound:

$$\min_{c^{-2}\in\mathcal{W}_N;\ h\in\mathbb{R}^N,\ \|h\|_{L^\infty(\Omega)}=1} \|DF_\omega[c^{-2}]h\|_* \geq \omega^2 e^{-K(1+\omega^2 B_2)\left(\frac{|\Omega|}{r_0^3}\right)^{4/7}}, \tag{42}$$

where $K = K(L, A, r_1)$, and $\|\cdot\|_*$ indicates the norm in $\mathcal{L}(H^{1/2}(\partial\Omega), H^{-1/2}(\partial\Omega))$, i.e.,

$$\|T\|_* = \sup\{|\langle Tg, f\rangle| : g, f \in H^{1/2}(\partial\Omega), \|g\|_{H^{1/2}(\partial\Omega)} = \|f\|_{H^{1/2}(\partial\Omega)} = 1\}.$$

In fact, by the injectivity of DF_ω,

$$\min_{c^{-2}\in\mathcal{W}_N;\ h\in\mathbb{R}^N,\ \|h\|_{L^\infty(\Omega)}=1} \|DF_\omega[c^{-2}]h\|_* = m_0/2 > 0.$$

Then, there exists h_0 satisfying $\|h_0\|_{L^\infty(\Omega)} = 1$ and $c_0^{-2} \in \mathcal{W}_N$ such that

$$\|DF_\omega[c_0^{-2}]h_0\|_* \leq m_0 .$$

Hence, by the definition of $\|\cdot\|_*$, it follows that

$$\left|\langle DF_\omega[c_0^{-2}](h_0)g, f\rangle\right| = \left|\int_\Omega h_0 \tilde{u}_0 v_0\right| \leq m_0 \|\tilde{u}_0\|_{H^{1/2}(\partial\Omega)} \|v_0\|_{H^{1/2}(\partial\Omega)},$$

where $\tilde{u}_0$ and v_0 are solutions to the equation $(-\Delta - \omega^2 c_0^{-2})u = 0$ in Ω with boundary data g and f, respectively. Proceeding as in the proof of the stability result Proposition 10 and Remark 11, we derive that

$$1 = \|h_0^{-2}\|_{L^\infty(\Omega)} \leq \frac{1}{\omega^2} e^{K(1+\omega^2 B_2)\left(\frac{|\Omega|}{r_0^3}\right)^{4/7}} m_0,$$

which gives the lower bound (42).

Copyright © by SIAM. Unauthorized reproduction of this article is prohibited.

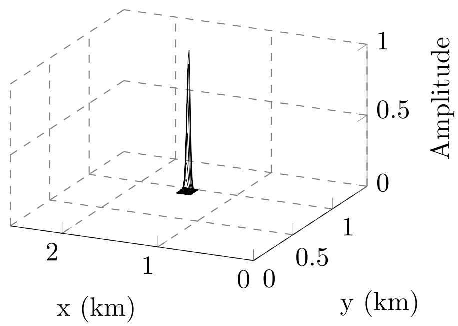

FIG. 1. *Illustration of the source shape for a localized boundary source.*

3. Computational experiments. In this section, we numerically compute the stability constant for the inverse problem associated with the Dirichlet-to-Neumann map. We illustrate the stability behaviour and compare it with the analytical bounds derived in section 2. The estimates we provide here are obtained from the definition of the stability constant,

$$\|c_1^{-2} - c_2^{-2}\|^2 < \mathcal{C}\|F_\omega(c_1^{-2}) - F_\omega(c_2^{-2})\|^2, \tag{43}$$

where $\|c_1^{-2} - c_2^{-2}\|$ denotes the L^2-norm of the functions from the finite-dimensional ansatz space. In particular, we consider here a geophysical example of reconstruction where normal data are collected on the boundary. In this situation c_1 and c_2 are assimilated to two different wavespeeds. Hence the boundary value problem (1) corresponds to the propagation of the acoustic wave in the media for a boundary source g using the wavespeeds c_1 and c_2, respectively. In our experiments, Gaussian-shaped (spatial) source functions (see Figure 1) are applied. Then the normal data (measurements of the normal derivative of the field) are acquired on the boundary in order to generate the forward operator. The numerical stability estimates are finally obtained by the knowledge of all quantities of (43).

In Remark 12, we have formulated the stability constant depending on the number of cubical partitions N in the model representation equation (40). This situation is well adapted for numerical applications where the domain is commonly discretized. Hence we want to verify the (exponential) dependence of the stability constant with N.

The model (assimilated to a wavespeed here) is defined on a cubical (structured) domain partition of a rectangular block. With increasing N, the size of the cubes decreases, possibly nonuniformly. We use piecewise constant functions on the cubes to define the wavespeeds following the main assumption for the Lipschitz stability to hold. Such a partition can be related to Haar wavelets, where N determines the scale. These naturally introduce approximate representations, that is, when the scale of the approximation is coarser than the finest scale contained in the model.

In order to solve the forward problem, the numerical discretization of the operator is realized using the discontinuous Galerkin method, where Dirichlet boundary conditions are invoked. The Dirichlet sources at the top boundary introduce an identity block in the discretized Helmholtz operator and give the following linear problem:

$$\begin{pmatrix} A_{ii} & A_{i\partial} \\ A_{\partial i} & A_{\partial\partial} \end{pmatrix} \begin{pmatrix} u_i \\ u_\partial \end{pmatrix} = \begin{pmatrix} A_{ii} & A_{i\partial} \\ 0 & Id \end{pmatrix} \begin{pmatrix} u_i \\ u_\partial \end{pmatrix} = \begin{pmatrix} 0 \\ g \end{pmatrix}, \tag{44}$$

Copyright © by SIAM. Unauthorized reproduction of this article is prohibited.

Downloaded 05/08/17 to 128.42.186.213. Redistribution subject to SIAM license or copyright; see http://www.siam.org/journals/ojsa.php

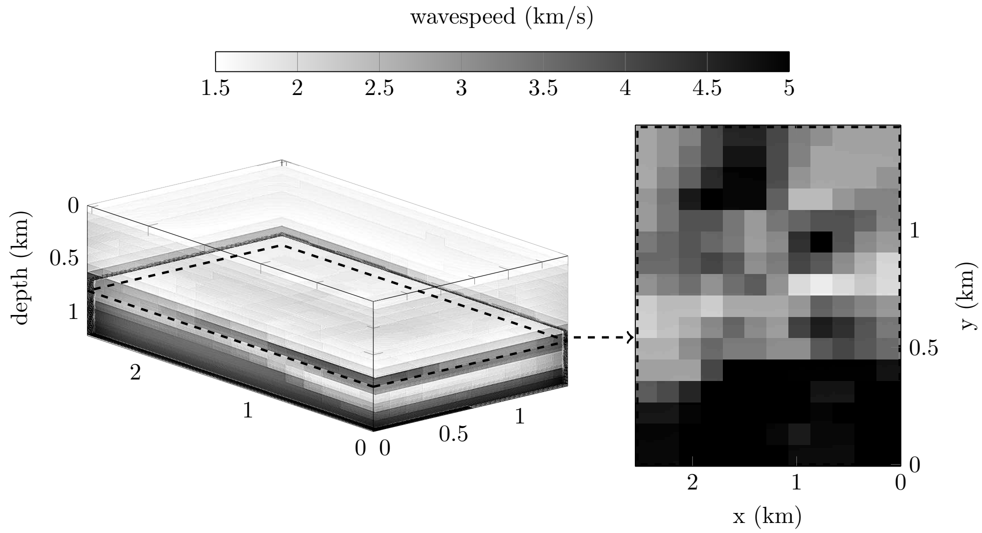

(a) Partition using $N = 2,880$ domains.

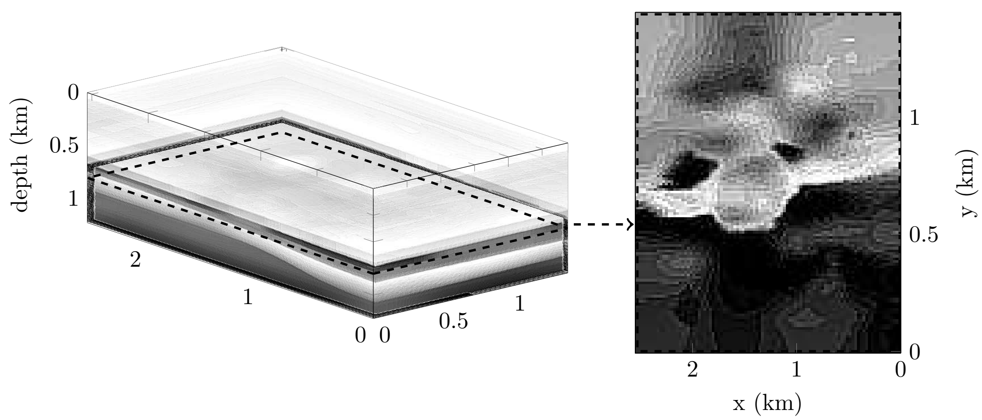

(b) Partition using $N = 1,527,168$ domains.

Fig. 2. *Three-dimensional representations and horizontal sections at* 800 *m depth of the reference wavespeed* (c_1) *using different partitions, i.e., scales. Every scale has a structured (rectangular) decomposition using piecewise constant functions. The size of the rectangular box defines the scale of the wavespeed (Courtesy of Statoil).*

where A represents the discretized operator, i labels the interior points and ∂ labels the boundary points, and g has values at the source location and is zero elsewhere. This system verifies $u_\partial = u_{|\partial\Omega} = g$ (i.e., the Dirichlet boundary condition) and $A_{ii}u_i + A_{i\partial}u_{|\partial\Omega} = 0$. The normal derivative data are generated by taking the normal derivative of the solution wavefield u on the surface.

Our experiments use a three-dimensional model of size $2.55 \times 1.45 \times 1.22$ km. The wavespeed c_1 is viewed as a reference model (which is known in this test case) and is represented in Figure 2. We also illustrate the different partitions of a model and the notion of approximation. Obviously, the larger the number of subdomains, the more precise the representation will be.

Copyright © by SIAM. Unauthorized reproduction of this article is prohibited.

Downloaded 05/08/17 to 128.42.186.213. Redistribution subject to SIAM license or copyright; see http://www.siam.org/journals/ojsa.php

Downloaded 05/08/17 to 128.42.186.213. Redistribution subject to SIAM license or copyright; see http://www.siam.org/journals/ojsa.php

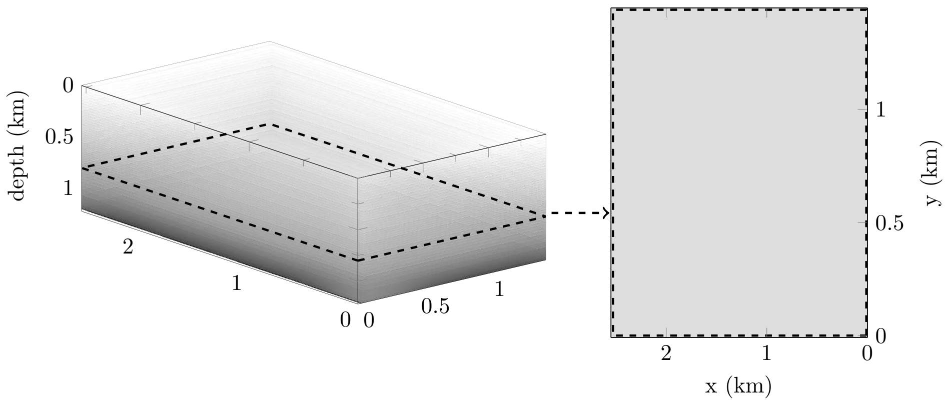

Fig. 3. *Three-dimensional wavespeed used for the successive estimation of the stability constant (c_2): 3D representation (left) and horizontal sections at 800 m depth (right).*

For the computation of the stability estimates, we consider c_2 as the model shown in Figure 3. This setup can be associated with the "true" subsurface in Figure 2 and the starting model in Figure 3. In this context we have chosen the initial guess with no knowledge of any structures by simply considering a one-dimensional variation in depth.

3.1. Estimates using the full Dirichlet-to-Neumann map. We consider the full data case where the Gaussian sources (see Figure 1) are positioned on each surface following a regular map. For each source, the data are acquired all over the boundary. We introduce a total of 630 sources and 76,538 data points for each.

At a selected partition (number of domains) and frequency, we simulate the data for the two media c_1 and c_2 and compute the difference, from which we deduce the stability constant following (43). The main difference with the standard seismic setup is that we consider data on all the boundary and not only at the top. This last case will be mentioned in subsection 3.2.

The numerical estimates for the stability constant $\mathcal{C}$ should depend on the number of domains N following the expression of the lower and upper bounds defined in Remark 12, (39), and (41). Thus we fix the frequency and estimate the stability for different partitions. The evolution of the estimates and underlying bounds are presented in Figure 4 at two selected frequencies, 5 and 10 Hz. We plot on a $\log\log$ scale the function $\log(\mathcal{C}\omega^2)$ to focus on the power of N in the estimates, which is the slope of the lines (4/7 for the upper bound and 1/5 for the lower bound).

Regarding the different coefficients in the analytical bounds, K and K_1 remain undecided and are numerically approximated so that the bounds match the estimates at best. For instance, the numerical value for K_1 is obtained from (39) by computing the average value based on the numerical stability estimates, and K is approximated following the same principle:

$$(45) \qquad K_1 = \frac{1}{n_{st}} \sum_{i=1}^{n_{st}} \frac{\log(4\omega^2 \mathcal{C}_i)}{N_i^{1/5}}, \qquad K = \frac{1}{n_{st}} \sum_{i=1}^{n_{st}} \frac{\log(\omega^2 \mathcal{C}_i)}{(1+\omega^2 B_2) N_i^{4/7}}.$$

Here, n_{st} is the number of numerical stability constant estimates and $\mathcal{C}_i$ is the corresponding estimate for partitioning N_i. We actually limit the computation of K to use only the first scales as it grows too rapidly. The numerical values obtained are

Copyright © by SIAM. Unauthorized reproduction of this article is prohibited.

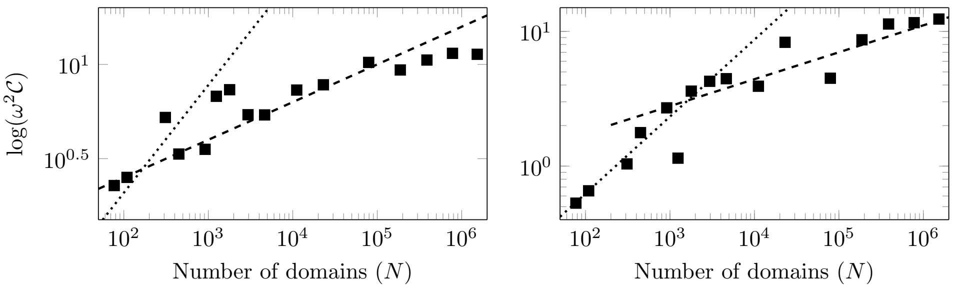

(a) Stability estimates at 5 Hz frequency. (b) Stability estimates at 10 Hz frequency.

FIG. 4. *The black squares represent the computational estimates of the stability constant (■) depending on the number of domains N at a selected frequency. The dashed line (- - -) represents the analytical lower bound and the dotted line (······) the upper bound, estimated with* (45).

FIG. 5. *The black squares represent the computational estimates of the stability constant (■) depending on the number of domains N at 10 Hz. The left part shows the coarsest scales which accurately match the upper bound (dotted line, ······). On the right, the finer scale estimates are accurately anticipated by the lower bound (dashed line, - - -). The constants K and K_1 for the computation of the lower and upper bounds are numerically approximated with the values given in Table* 1*, following* (45).

TABLE 1
Numerical estimation of the constant in the analytical bounds formulation for the numerical estimates of the stability (Figure 4*) with $B_2 = (1/1400)^2$.*

	5Hz	10Hz
K_1	1	0.7
K	0.15	0.05

given in Table 1. We also note that the term $\omega^2 B_2$ of the upper bound equation (41) is relatively small in the geophysical context we have here, $B_2 = 5.10^{-7}$.

We can see that the stability constant increases with the number of subdomains, as expected. There are clearly two states in the evolution of the estimates at the highest frequency (10 Hz, Figure 4(b)). For a low number of partitions N the numerical estimates match the upper bound particularly well, while at finer scales it follows the lower bound accurately. This is illustrated in Figure 5 where we decompose the two parts of the estimates between the low and high numbers of domains.

Copyright © by SIAM. Unauthorized reproduction of this article is prohibited.

Downloaded 05/08/17 to 128.42.186.213. Redistribution subject to SIAM license or copyright; see http://www.siam.org/journals/ojsa.php

Downloaded 05/08/17 to 128.42.186.213. Redistribution subject to SIAM license or copyright; see http://www.siam.org/journals/ojsa.php

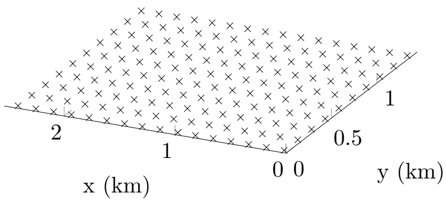

(a) The crosses represent the boundary source locations.

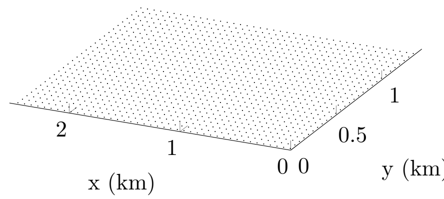

(b) The lattice represents the discretization of the data, i.e., the locations of receivers.

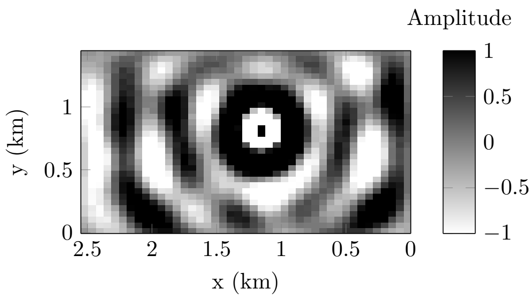

(c) Data recovered from a boundary centered shot, i.e., wavefield measured at the locations of the receivers.

FIG. 6. *Illustration of the seismic acquisition set.*

Alternatively, for a lower frequency, i.e., 5 Hz on Figure 4(a), the upper bound appears to increase too rapidly, while the lower bound accurately matches the evolution of the stability constant estimates. Hence the upper bound we have obtained here is particularly appropriate for coarse scale and high frequency, when the variation of the model is much coarser compared to the wavelength.

3.2. Seismic inverse problem using partial data. In realistic geophysical experiments for the reconstruction of subsurface area (seismic tomography), it is more appropriate not to consider the full data but only the partial data located on the upper surface. The data obtained from c_1 can be seen as a field observation (sensor measurement of a seismic event at the surface). The data using c_2 are a simulation using an "initial guess." For the reconstruction, we mention the full waveform inversion method, where the recovery follows an iterative minimization of the difference between the measurements and the simulations to successively update the initial guess (see [23, 20]). There is also the difference in the boundary conditions where perfectly matched layers or absorbing boundary conditions are invoked instead of the Dirichlet boundary condition for the lateral and bottom boundaries. However, the top boundary is a free surface and remains a Dirichlet boundary condition.

For this test case, we reproduce the same experiments but limit the set of sources and the collected data to be at the top boundary only. We define a set of sources at the surface, separated by 160 m along the x-axis and 150 m along the y-axis to generate a regular map of 16×10 points. The receivers (data location) are positioned in the same fashion every 60 m along the x-axis and 45 m along the y-axis and generate a regular map of 43×32 points; see Figures 6(a) and 6(b). The partial boundary data computed are illustrated for a single centered boundary shot at 5 Hz frequency; see Figure 6(c).

Copyright © by SIAM. Unauthorized reproduction of this article is prohibited.

Downloaded 05/08/17 to 128.42.186.213. Redistribution subject to SIAM license or copyright; see http://www.siam.org/journals/ojsa.php

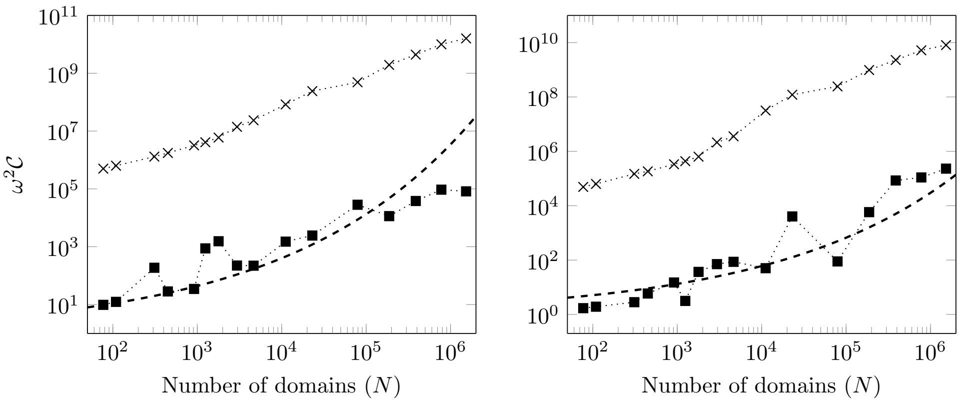

(a) Stability estimates at 5 Hz frequency.

(b) Stability estimates at 10 Hz frequency.

Fig. 7. *Comparison of the computational stability estimates using partial data only located on the top boundary* ($\cdots\times\cdots$) *and using the full boundary data* ($\cdots\blacksquare\cdots$). *The dashed line* (- - -) *represents the analytical lower bound as found in Figure* 4.

In Figure 7 we compare the stability constant estimates using partial data with the stability constant estimates obtained when considering the full Dirichlet-to-Neumann map as the data. We incorporate the analytical lower bound that was computed in the previous test case.

The numerical estimates of the stability constants for the full and partial data in a log log scale differ by a constant. This leads us to our conjecture that the log log of the stability constants (as a function of N) of the full and partial data case in the continuous setting differ by a constant.

Acknowledgment. This research was supported in part by the members BGP, ExxonMobil, PGS, Statoil, and Total of the Geo-Mathematical Imaging Group now at Rice University. We want to thank the referees for their valuable comments and suggestions, which significantly contributed to improving the quality and clarity of the paper.

REFERENCES

[1] G. Alessandrini, *Stable determination of conductivity by boundary measurements*, Appl. Anal., 27 (1988), pp. 153–172, doi:10.1080/00036818808839730.

[2] G. Alessandrini and S. Vessella, *Lipschitz stability for the inverse conductivity problem*, Adv. Appl. Math., 35 (2005), pp. 207–241, doi:10.1016/j.aam.2004.12.002.

[3] G. Bao and P. Li, *Inverse medium scattering problems for electromagnetic waves*, SIAM J. Appl. Math., 65 (2005), pp. 2049–2066, doi:10.1137/040607435.

[4] G. Bao and F. Triki, *Error estimates for the recursive linearization of inverse medium problems*, J. Comput. Math., 28 (2010), pp. 725–744, doi:10.4208/jcm.1003-m0004.

[5] H. Ben-Hadj-Ali, S. Operto, and J. Virieux, *Velocity model-building by 3d frequency-domain, full-waveform inversion of wide-aperture seismic data*, Geophysics, 73 (2008), VE101, doi:10.1190/1.2957948.

[6] E. Beretta, M. V. de Hoop, and L. Qiu, *Lipschitz stability of an inverse boundary value problem for a Schrödinger-type equation*, SIAM J. Math. Anal., 45 (2013), pp. 679–699, doi:10.1137/120869201.

[7] E. Beretta and E. Francini, *Lipschitz stability for the electrical impedance tomography problem: The complex case*, Comm. Partial Differential Equations, 36 (2011), pp. 1723–1749, doi:10.1080/03605302.2011.552930.

[8] K. D. Blazek, C. Stolk, and W. W. Symes, *A mathematical framework for inverse wave problems in heterogeneous media*, Inverse Problems, 29 (2013), 065001, doi:10.1088/0266-5611/29/6/065001.

Copyright © by SIAM. Unauthorized reproduction of this article is prohibited.

[9] K. Datchev and M. V. de Hoop, *Iterative Reconstruction of the Wavespeed for the Wave Equation with Bounded Frequency Boundary Data*, preprint, arXiv:1506.09014, 2015.

[10] E. B. Davies, *Spectral Theory and Differential Operators*, Cambridge Studies in Advanced Mathematics 42, Cambridge University Press, Cambridge, 1995, doi:10.1017/CBO9780511623721.

[11] J. Feldman, M. Salo, and G. Uhlmann, *The Calderón Problem—An Introduction to Inverse Problems*, 2015, http://www.math.ubc.ca/~feldman/ibook/.

[12] D. Gilbarg and N. S. Trudinger, *Elliptic Partial Differential Equations of Second Order*, Grundlehren der Mathematischen Wissenschaften [Fundamental Principles of Mathematical Sciences] 244, 2nd ed. Springer-Verlag, Berlin, 1983.

[13] P. Hähner, *A periodic Faddeev-type solution operator*, J. Differential Equations, 128 (1996), pp. 300–308, doi:10.1006/jdeq.1996.0096.

[14] P. Hähner and T. Hohage, *New stability estimates for the inverse acoustic inhomogeneous medium problem and applications*, SIAM J. Math. Anal., 33 (2001), pp. 670–685, doi:10.1137/S0036141001383564.

[15] T. Hohage, *Logarithmic convergence rates of the iteratively regularized Gauss - Newton method for an inverse potential and an inverse scattering problem*, Inverse Problems, 13 (1997), pp. 1279–1299, doi:10.1088/0266-5611/13/5/012.

[16] R. Magnanini and G. Papi, *An inverse problem for the Helmholtz equation*, Inverse Problems, 1 (1985), pp. 357–370, doi:10.1088/0266-5611/1/4/007.

[17] N. Mandache, *Exponential instability in an inverse problem for the Schrödinger equation*, Inverse Problems, 17 (2001), pp. 1435–1444, doi:10.1088/0266-5611/17/5/313.

[18] S. Nagayasu, G. Uhlmann, and J.-N. Wang, *Increasing stability in an inverse problem for the acoustic equation*, Inverse Problems, 29 (2013), 025012, doi:10.1088/0266-5611/29/2/025012.

[19] R. G. Novikov, *New global stability estimates for the Gel'fand-Calderon inverse problem*, Inverse Problems, 27 (2011), 015001, doi:10.1088/0266-5611/27/1/015001.

[20] R. G. Pratt, C. Shin, and G. J. Hicks, *Gauss-Newton and full Newton methods in frequency-space seismic waveform inversion*, Geophys. J. Internat., 133 (1998), pp. 341–362, doi:10.1046/j.1365-246X.1998.00498.x.

[21] J. Sylvester and G. Uhlmann, *A global uniqueness theorem for an inverse boundary value problem*, Ann. Math. (2), 125 (1987), pp. 153–169, doi:10.2307/1971291.

[22] W. W. Symes, *The seismic reflection inverse problem*, Inverse Problems, 25 (2009), 123008, doi:10.1088/0266-5611/25/12/123008.

[23] A. Tarantola, *Inversion of seismic reflection data in the acoustic approximation*, Geophysics, 49 (1984), pp. 1259–1266.

Downloaded 05/08/17 to 128.42.186.213. Redistribution subject to SIAM license or copyright; see http://www.siam.org/journals/ojsa.php

Copyright © by SIAM. Unauthorized reproduction of this article is prohibited.